

Fast wave power flow along SOL field lines in NSTX

R.J. Perkins¹, J.-W. Ahn², R. E. Bell¹, A. Diallo¹, S. Gerhardt¹, T. K. Gray², D. L. Green², E. F. Jaeger², J. C. Hosea¹, M. A. Jaworski¹, B. P. LeBlanc¹, G. J. Kramer¹, A. McLean², R. Maingi², C. K. Phillips¹, L. Roquemore¹, P. M. Ryan², S. Sabbagh³, G. Taylor¹, J. R. Wilson¹

¹PPPL, Princeton University, Princeton, NJ 08540, USA

²ORNL, Oak Ridge, TN 37831, USA

³Columbia University, New York, NY 10027, USA

It is found that, on NSTX, a major loss of high-harmonic fast wave (HHFW) power can occur along open field lines passing in front of the antenna (Fig. 1) over the width of the scrape-off layer (SOL). This loss differs considerably from the well-studied losses occurring directly at the antenna components [1,2], which can cause impurity release into the plasma [3,4], and is likely the cause of the erosion in the divertor found on C-mod [5]. Importantly, this loss of RF power must be subtracted from the coupled power before multipass damping is considered. That is, the efficiency should be calculated as $P_{\text{dep}}/P_{\text{RF}} = (1 - \Delta_{\text{SOL}}) * \eta_{\text{sing}}/(\eta_{\text{sing}} + \eta_{\text{edge}})$, where Δ_{SOL} , η_{sing} , and η_{edge} are the damping fractions in the first pass of the SOL (including power losses at the antenna and divertor regions), crossing the core plasma, and at the cutoff layer zone, respectively. Fully understanding the underlying mechanisms behind this loss is critical for optimizing HHFW performance and fast wave performance generally. This is especially important for optimizing high-power long-pulse ICRF heating on ITER while guarding against excessive erosion in the divertor region.

Experimental observations suggest that the edge-loss of RF power on NSTX is significant and that this lost power, in part, flows from the antenna vicinity along field lines to the divertor regions. Up to 60% of the RF power can be lost to the SOL regions and at least partially deposited in bright spirals on the divertor floor and ceiling (Fig. 1); the heat flux to the lower spiral can be up to 2 MW/m² for 2

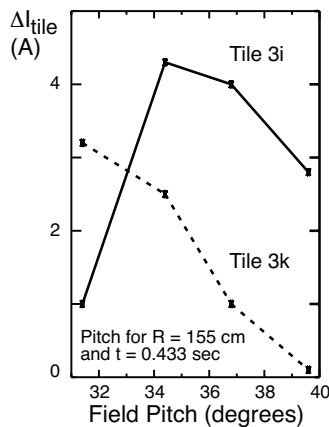


Figure 2. RF-induced currents to tiles 3i and 3k versus field pitch in front of the antenna. ($k_{\parallel} = -8\text{m}^{-1}/\phi_{\text{Ant}} = -90^\circ$, D_2 , $P_{\text{NB}} = 2\text{ MW}$.)

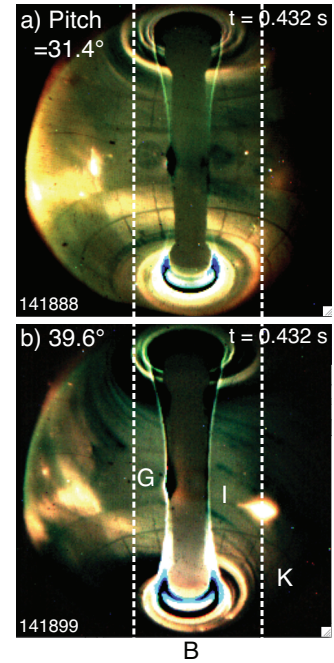


Figure 1. RF power is channeled from the antenna to the divertor through the SOL. a) Low magnetic pitch shot (31° at antenna); b) high pitch shot (40°). Antenna is on left and Bay B, G, I and K locations are indicated.

MW of applied HHFW power [6,7]. The RF spiral is observed to move across the divertor as the magnetic field pitch in NSTX is varied; in Fig. 1, the spiral radius decreases with pitch at any given toroidal location by up to 15 cm. Also, when the spiral lies over a diagnostic, that diagnostic is found to respond strongly to the RF pulse. For instance, the RF-induced currents to certain divertor tiles depend strongly on the magnetic pitch (Fig. 2) because changing the pitch moves the spiral onto and off of these tiles. Likewise, at the highest pitch, the spiral is pushed partly over a four-probe radial array; the floating potential of probe 4, the outermost probe, is driven to negative values during the RF pulse (Fig. 3) whereas the signal of probe 2, just 6 cm inboard of probe 4, is little affected, showing that the RF effect on the probes is localized to within the spiral.

Mapping magnetic field lines from the SOL midplane to the divertor elucidates the above observations provided that the mapping

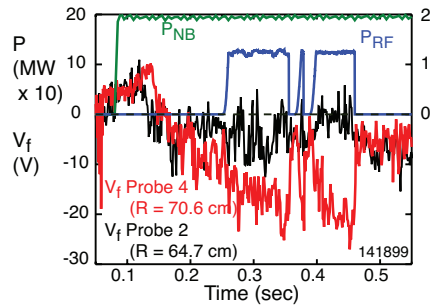


Figure 3. Probe 4 of the probe array responds to the RF at the highest pitch as the spiral over it. Probe 2, 6 cm inboard and not fully under the spiral, shows almost no response to the RF.

includes field lines across the SOL in front of the antenna. Figure 4 plots the points where field lines originating from the SOL midplane strike the lower divertor for the two pitch cases of Fig. 1. The field lines begin at midplane radii values R_{SOL} from 157.5 cm (the major radius of the Faraday screen) to 152 cm (just outside the last closed flux surface) in increments of 0.25 cm; the particles are color-coded to denote their starting radii. Field lines starting closer to the LCFS strike the divertor farther in radially and wrap around the center column more toroidally so that the set of strike points defines a spiral in agreement with the visible-camera images. Figure 4 captures the movement of the spiral as the pitch increases and reveals that this movement results from a counter-clockwise rotation of the spiral. Figure 4 also explains the response of the tile currents and Langmuir probes to the application of RF power as a function of magnetic pitch. At higher pitch, the spiral moves off of tile 3k and onto tile 3i and the outermost probes in agreement with the data.

Thus, the flow of RF power in the SOL to the divertor regions is aligned along the magnetic field and furthermore, the RF power is deposited across the SOL in front of the antenna instead of solely at the Faraday screen and limiters. We hypothesize that surface waves are being excited just beyond the fast wave perpendicular onset density and note that the location at which the plasma density exceeds the onset density for perpendicular wave propagation typically occurs a few cm away from the antenna [8,9], a location possibly consistent with the field-line mapping. Whatever the underlying mechanism though, these results should serve to benchmark advanced code simulations of the RF edge power deposition in the SOL (e.g., [11]) to give power flow along the open field lines passing in front of the antenna. These codes can then be combined with edge RF field measurements to predict and minimize such edge losses in the ion cyclotron range of frequencies (ICRF) heating regime.

This work was supported by DOE Contract No. DE-AC02-09CH11466.

- [1] P. Jacquet *et al.*, *Nuclear Fusion* **51** (2011) 103018 (and references therein).
- [2] L. Colas *et al.*, *AIP Conf Proceedings* **787** (2005) 150.
- [3] J.E. Stevens *et al.*, *Plasma Physics and Controlled Fusion* **32** (1990) 189.
- [4] M. Bures *et al.*, *Plasma Physics and Controlled Fusion* **33** (1991) 937.
- [5] S.J. Wukitch *et al.*, *AIP Conf Proceedings* **933** (2007) 75.
- [6] J.C. Hosea *et al.*, *AIP Conf Proceedings* **1187** (2009) 105.
- [7] G. Taylor *et al.*, *Physics of Plasmas* **17** (2010) 056114.
- [8] J.C. Hosea *et al.*, *Physics of Plasmas* **15** (2008) 056104.
- [9] C.K. Phillips *et al.*, *Nuclear Fusion* **49** (2009) 075015.
- [10] J.C. Hosea *et al.*, *AIP Conf Proceedings* **1406** (2011) 333.
- [11] D.L. Green *et al.*, *Physical Review Letters* **107** (2011) 145001.

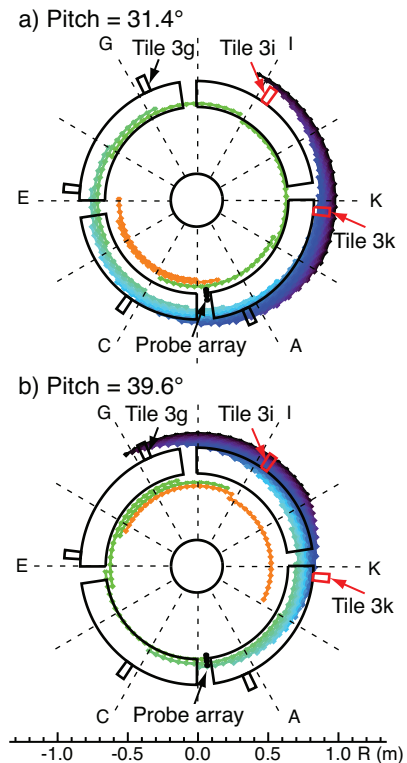


Figure 4. The field-line strike points on the bottom divertor vs field pitch for $t = 0.433$ sec. The starting radii of the field lines at the midplane span the SOL, varying between 157.5 cm and 152 cm (antenna radius = 157.5 cm and last closed flux surface radius ≈ 152 cm).